

# Ringlike structures in the density–magnetic-field $\rho_{xx}$ diagram of two-subband quantum Hall systems

Gerson J. Ferreira<sup>\*1</sup>, Henrique J. P. Freire<sup>1</sup>, and J. Carlos Egues<sup>1,2</sup>

<sup>1</sup> Instituto de Física de São Carlos, Universidade de São Paulo,  
Caixa Postal 369, 13560-590 São Carlos, SP, Brazil

<sup>2</sup> Department of Physics and Astronomy, University of Basel, CH-4056 Basel, Switzerland

**Key words** quantum hall ferromagnetism, density functional theory, two-subband quantum wells

**PACS** 71.15.Mb, 73.43.-f

Motivated by recent experiments [Zhang *et al.*, Phys. Rev. Lett. **95**, 216801 (2005) and Ellenberger *et al.*, cond-mat/0602271] reporting novel ringlike structures in the density–magnetic-field ( $n_{2D}$ – $B$ ) diagrams of the longitudinal resistivity  $\rho_{xx}$  of quantum wells with two subbands, we investigate theoretically here the magneto-transport properties of these quantum-Hall systems. We determine  $\rho_{xx}$  via both the Hartree and the Kohn-Sham self-consistent schemes plus the Kubo formula. While the Hartree calculation yields diamond-shaped structures in the  $n_{2D}$ – $B$  diagram, the calculation including exchange and correlation effects (Kohn-Sham) more closely reproduces the ringlike structures in the experiments.

Copyright line will be provided by the publisher

## 1 Introduction

Quantum Hall systems, i.e., two-dimensional electron gases (2DEGs) under strong magnetic fields, exhibit a variety of novel physical phenomena [1]. Besides the widely known quantum Hall effects, these systems also display quantum Hall ferromagnetism – an spontaneously formed spin-polarized many-body state arising from the interplay of the Zeeman, Coulomb, and thermal energy scales within the highly-degenerate Landau states of the 2DEG [2].

Quantum Hall ferromagnetism has been experimentally investigated via magneto-transport measurements of the longitudinal  $\rho_{xx}$  and Hall  $\rho_{xy}$  resistances in both the integer and fractional quantum Hall regimes. A crucial ingredient in these experiments is the occurrence of opposite-spin Landau level crossings [3] near the Fermi energy. At these crossings the system may find it energetically favorable to spin polarize thus reducing its energy due to the Pauli-Coulomb exchange interaction. Resistance spikes (or “anomalous” peaks) are found in  $\rho_{xx}$  at these crossings. Corresponding dips or bumps in  $\rho_{xy}$  are sometimes reported. Most importantly, these features in  $\rho_{xx}$  and  $\rho_{xy}$  are hysteretic in many cases thus signaling Ising-like ferromagnetism [4, 5, 6, 7].

Recent experiments in two-subband quantum Hall systems [8, 9] have found interesting ringlike structures (Fig. 1(a), reproduced from Ref. [8]) in the density–magnetic-field ( $n_{2D}$ – $B$ ) diagram of  $\rho_{xx}$ . The authors of Ref. [8] claim that these unusual structures arise from quantum Hall ferromagnet states in the system, while those of Ref. [9] explain their ringlike structures in terms of a phenomenological single-particle picture. In both experiments crossings of Landau levels from distinct confined subbands occur at the Fermi level.

Here we theoretically investigate the magneto-transport properties of quantum-Hall systems with two occupied subbands. We consider a modulation-doped GaAs/AlGaAs quantum well, similar to that of Ref. [8],[10]. We determine the subband structure of the well via both (i) the Hartree approach and (ii) the

<sup>\*</sup> Corresponding author: e-mail: gersonjr@ifsc.usp.br

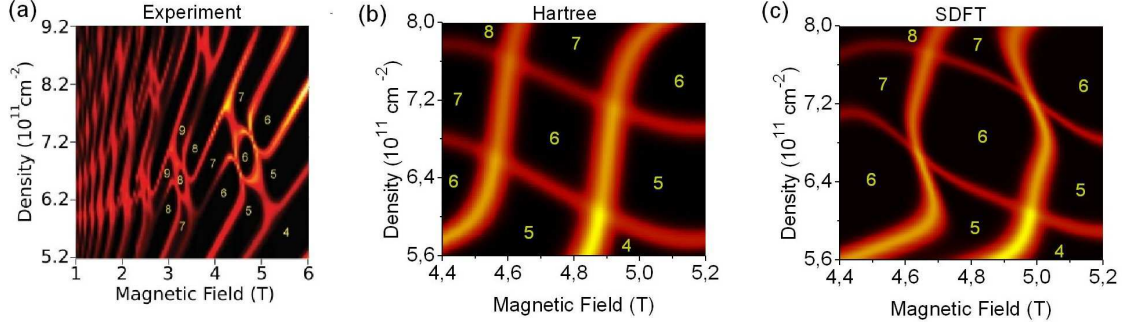


**Fig. 1** Experimental (a) (adapted from Ref. [8]) and calculated density-magnetic-field  $\rho_{xx}$  diagrams within the Hartree approximation (b) and the SDFT/LSDA (c). Only the ringlike structure corresponding to filling factor  $\nu = 6$  is shown in (b) and (c).

Spin Density Functional Theory (SDFT) [11] [within the Local Spin density Approximation (LSDA)] implemented via the usual Kohn-Sham scheme [12]. We obtain the magneto-conductivity tensor (and its inverse, the magneto-resistivity) from the Kubo formula. We find diamond-shaped structures [Fig. 1(b)] in the  $n_{2D}$ - $B$  diagram within the Hartree approximation, while the SDFT-LSDA calculation yields smoother structures [Fig. 1(c)] more closely resembling the ringlike shapes in Refs. [8, 9] [e.g., Fig. 1(a)]. We do not find any hysteresis or discontinuities in the DFT-LSDA Landau-level fan diagram, which would indicate easy-axis (Ising) quantum Hall ferromagnetism in the system [4, 5, 6, 7]. However, we can not rule out the possibility for easy-plane ferromagnetism.

## 2 Self-consistent approach

*Hartree and SDFT/LSDA calculations.* Within the usual implementation of the SDFT/LSDA formulation in the context of the effective mass approximation, we self-consistently solve the Kohn-Sham equations for the conduction electrons in an external potential. Because of the translational symmetry in the  $xy$  plane of the 2DEG, the problem is separable [7]. For the  $z$  direction we have two (spin up and down) coupled one-dimensional Schrödinger equations

$$\left[ -\frac{\hbar^2}{2m} \frac{d}{dz^2} + v_{eff}^{\sigma_z}(z; [n_{\uparrow}, n_{\downarrow}]) \right] \chi_i^{\sigma_z}(z) = \varepsilon_i^{\sigma_z} \chi_i^{\sigma_z}(z), \quad (1)$$

with  $m$  being the effective mass,  $i = 1, 2, \dots$  the subband index, and  $v_{eff}^{\sigma_z}(z)$  the effective single-particle potential. While the heterostructure potential confines the longitudinal motion, the perpendicular magnetic field collapses the transversal motion into Landau levels with energies  $\varepsilon_n = (n + 1/2)\hbar\omega_c$ ,  $\omega_c = eB/m$ , each of which with a macroscopic degeneracy  $eB/h$  ( $\sim 10^{11} \text{ cm}^{-2}$ ). Therefore, the Kohn-Sham single-particle energy of each electronic level is

$$\varepsilon_{i,n}^{\sigma_z} = \varepsilon_i^{\sigma_z} + \left( n + \frac{1}{2} \right) \hbar\omega_c + \frac{\sigma_z}{2} g\mu_B B. \quad (2)$$

where  $g\mu_B B\sigma_z/2$  is the ordinary Zeeman term and  $g$  the effective Landé factor. The spin-dependent effective potential in Eq. (1) consists of two main contributions: the confining potential of the heterostructure  $v_c(z)$  and the Coulomb potential which in the Kohn-Sham/SDFT scheme is split into Hartree  $v_H(z, [n])$  and an exchange-correlation (XC)  $v_{xc}(z, [n_{\uparrow}, n_{\downarrow}])$  contributions. The one-dimensional effective potential in the  $z$ -direction then reads

$$v_{eff}^{\sigma_z}(z, [n_{\uparrow}, n_{\downarrow}]) = v_c(z) + v_H(z, [n]) + v_{xc}^{\sigma_z}(z, [n_{\uparrow}, n_{\downarrow}]). \quad (3)$$

In our simulations, the structural potential  $v_c(z)$  represents the square quantum well investigated in Ref. [8]. The Hartree potential is calculated by solving the Poisson's equation taking into account the electronic charge density *and* the positive charge profile of the depleted modulation-doped regions. For the XC potential we use the Vosko-Wilk-Nusair (VWN) [13] parameterization of the LSDA.

Since  $v_H$  and  $v_{xc}$  are both functionals of  $n_\uparrow$  and  $n_\downarrow$ , which are calculated from the Kohn-Sham orbitals  $\chi_i^{\sigma_z}(z)$ , Eqs. (1) and (3) are solved self-consistently. The densities, and any other observable of interest, are calculated using a Gaussian broadened density of states (DOS) weighed by the Fermi function (*aufbau* principle). Each level is characterized by a width  $\Gamma^{\sigma_z}$  with an electron density  $eB/h$ . Note that the Hartree calculation is obtained from the above self-consistent scheme by simply turning off the XC contribution.

*Magneto-transport.* We determine the magneto-resistances from the magneto-conductivity tensor ( $\rho = \sigma^{-1}$ ), calculated within the self-consistent Born-approximation model of Ando and Uemura [14, 15]. For short-range scatterers,

$$\sigma_{xx} = \frac{4e^2}{h} \int_{-\infty}^{\infty} \left( -\frac{\partial f(\varepsilon)}{\partial \varepsilon} \right) \sum_{i,n,\sigma_z} \left( n + \frac{1}{2} \right) \exp \left[ -\left( \frac{\varepsilon - \varepsilon_{i,n}^{\sigma_z}}{\Gamma_{\text{ext}}} \right)^2 \right] d\varepsilon \quad (4)$$

where  $\sigma_{xy} = en_{2D}/B + \Delta\sigma_{xy}$  with  $\Delta\sigma_{xy}$  being a small correction [14, 15]. We model the extended Landau states by a Gaussian DOS  $g_{\text{ext}}(\varepsilon)$  of width  $\Gamma_{\text{ext}} = 0.25$  meV [16]. Next we present our results.

### 3 Results and discussions

*Parameters.* We consider a GaAs/Al<sub>0.3</sub>Ga<sub>0.7</sub>As modulation-doped quantum well [8] with a width  $L = 240$  Å and two symmetric  $\delta$ -doped layers with planar density  $n_{2D} = 10^{12}$  cm<sup>-2</sup> (which is identical to the electron density in our simulations), set back from the well by 240 Å. We use an effective g-factor  $g = -0.44$ ,  $m = 0.063$ , a potential well offset  $\sim 236.43$  meV [17, 18] and  $T = 340$  mK [8] in our simulations.

*Hartree calculation.* First of all we note that in a Hartree-type calculation the Zeeman interaction is the only source of the spin splitting of the energy levels. Moreover, this splitting increases linearly with  $B$  and does not depend on the electron density  $n_{2D}$ . Using standard parameters for GaAs wells, *e.g.*  $g = -0.44$  and  $m = 0.063$ , our Hartree calculation yields  $n_{2D}$ - $B$   $\rho_{xx}$  diagrams showing small diamond-shaped structures (this shape follows from the linear dependence of the spin splitting with  $B$ ) while the experiment [8] exhibits much larger ring-like structures [Fig. 1(a)]. In order to generate structures with an area comparable to the experimental rings, we need to use an enhanced  $g \sim -2.1$  in our Hartree simulation. This value is consistent with the experimental estimate of Ellenberger *et al.* [9] who correctly suggests (as our SDFT/LSDA calculation below shows) that this enhancement is due to exchange-correlation effects. Figure 1(b) shows the  $\nu = 6$  diamond. The small area of the diamonds calculated with the standard parameters suggests that the Zeeman effect is not the only source of spin splitting in the experiments. This is indeed the case, as we find in the SDFT/LSDA calculation.

*SDFT/LSDA calculation.* Here, in contrast to the Hartree case, the spin-dependent exchange-correlation potential  $v_{xc}^{\sigma_z}(z, [n_\uparrow, n_\downarrow])$  in the Kohn-Sham equations gives rise to a density-dependent spin splitting, not linear in  $B$ . Figure 1(c) shows the  $\nu = 6$  structure in the  $n_{2D}$ - $B$  diagram, calculated via the SDFT/LSDA with standard parameters for GaAs wells. We can see a smoother structure which more closely resembles the ring-like structures in the experiment of Ref. [8] [Fig. 1(a)]. We have also calculated the full range  $n_{2D}$ - $B$   $\rho_{xx}$  diagram and find that it is very similar to the experimental one, Fig. 1(a) [19]. Therefore, the SDFT-type calculation with the standard GaAs parameters results in more rounded structures with areas and shapes similar to those reported in Refs. [8] and [9].

*Quantum Hall ferromagnetism.* The above results seem to corroborate the conjecture in Ref. [8] that the ringlike shapes of the structures should be due to density-dependent exchange-correlation effects. However, our SDFT/LSDA simulations do not show ferromagnetic phase transitions. The Landau fan diagram

and the resistivities ( $\rho_{xx}$  and  $\rho_{xy}$ ) do not show any hysteresis or discontinuities which would signal an easy-axis (Ising-like) ferromagnetic transition [4, 5, 6, 7]. In addition, the spin-polarization at the center of the rings are too small to be understood as an easy-axis ferromagnetic phase. However, we cannot rule out easy-plane ( $xy$ ) ferromagnetism. In fact, an early experimental investigation [20] has reported on the observation of both easy-axis and easy-plane quantum-Hall ferromagnetism in similar systems.

## 4 Summary

We have calculated the  $n_{2D}$ - $B$  diagram of  $\rho_{xx}$  within both the Hartree and the SDFT/LSDA approaches (plus the Kubo formula) in two-subband quantum Hall systems. While our Hartree calculation with an artificially enhanced  $g$  factor of  $-2.1$  yields diamond-shaped structures, the calculation with density- and spin-dependent exchange-correlation effects and the standard  $g = -0.44$  value, more closely reproduces the ringlike shapes seen experimentally.

**Acknowledgements** GJF thanks X. Zhang for providing some experimental details. JCE acknowledges useful discussions with K. Ensslin. This work was supported by CNPq and FAPESP.

## References

- [1] *Perspectives on Quantum Hall effects*, edited by S. Das Sarma and A. Pinczuk (Wiley, New York, 1997).
- [2] G. F. Giuliani and J. J. Quinn, Phys. Rev. B **31**, 6228 (1985); S. M. Girvin and A. H. MacDonald in Ref. [1].
- [3] F. F. Fang and P. J. Stiles, Phys. Rev. **174**, 823 (1968).
- [4] V. Piazza, V. Pellegrini, F. Beltram, W. Wegscheider, T. Jungwirth, and A. H. MacDonald, Nature **402**, 638 (1999).
- [5] T. Jungwirth and A. H. MacDonald, Phys. Rev. Lett. **87**, 216801 (2001).
- [6] J. Jaroszyński, T. Andrearczyk, G. Karczewski, J. Wróbel, T. Wojtowicz, E. Papis, E. Kamińska, A. Piotrowska, Dragana Popović, and T. Dietl, Phys. Rev. Lett. **89**, 266802 (2002).
- [7] Henrique J. P. Freire and J. Carlos Egues, cond-mat/0412491.
- [8] X. C. Zhang, D. R. Faulhaber, and H. W. Jiang, Phys. Rev. Lett. **95** 216801, (2005); see also X. C. Zhang, I. Martin, and H. W. Jiang, cond-mat/0607208.
- [9] C. Ellenberger, B. Simovic, R. Leturcq, T. Ihn, S.E. Ulloa, K. Ensslin, D. C. Driscoll, and A. C. Gossard, cond-mat/0602271.
- [10] Preliminary simulations for the parabolic well of Ref. [9] show qualitative similar results as described here.
- [11] P. Hohenberg and W. Kohn, Phys. Rev. **136**, B864 (1964).
- [12] W. Kohn and L. J. Sham, Phys. Rev. **140**, A1133 (1965).
- [13] S. H. Vosko, L. Wilk, and M. Nusair, Can. J. Phys. **58**, 1200 (1980).
- [14] T. Ando and Y. Uemura, J. Phys. Soc. Jpn. **36**, 959 (1974).
- [15] Tsuneya Ando, J. Phys. Soc. Jpn. **37**, 622 (1974).
- [16] R. E. Prange, Phys. Rev. B **23**, 4802 (1981).
- [17] O. Madelung, M. Schulz and H. Weiss, eds., *Semiconductors*, vol. 17 of *Landolt-Börnstein: Numerical Data and Functional Relationships in Science and Technology, New Series, Group III: Crystal and Solid State Physics* (Springer, Berlin, 1982).
- [18] I. Vurgaftman, J. R. Meyer, and L. R. Ram-Mohan, J. Appl. Phys. **89**, 5815 (2001).
- [19] We note that the shape of the lines connecting the  $\nu = 6$  and the  $\nu = 4$  regions in Fig. 1 [see “necks” in Fig. 1(a) and the crossings in Figs. 1(b) and 1(c)] depends crucially on the DOS used (e.g., Lorentzian or Gaussian) and the broadening of the Landau levels. This will be discussed in detail elsewhere (Ferreira, Freire and Egues, in preparation).
- [20] Koji Muraki, Tadashi Saku, and Yoshiro Hirayama, Phys. Rev. Lett. **87**, 196801 (2001).

This figure "fig1.jpg" is available in "jpg" format from:

<http://arxiv.org/ps/cond-mat/0607456v2>

This figure "fig1.png" is available in "png" format from:

<http://arxiv.org/ps/cond-mat/0607456v2>